Journal of the European Ceramic Society 22 (2002) 2379–2387

www.elsevier.com/locate/jeurceramsoc

Compositional identification of the intergranular phase in liquid phase sintered SiC

Haihui Ye*, Georg Rixecker, Siglinde Haug, Fritz Aldinger

Max-Planck-Institut für Metallforschung and Institut für Nichtmetallische Anorganische Materialien, Universität Stuttgart, Pulvermetallurgisches Laboratorium, Heisenbergstrasse 5, D-70569 Stuttgart, Germany

Received 28 May 2001; received in revised form 5 December 2001; accepted 28 December 2001

Abstract

A model system consisting of coarse SiC (32–160 μm) as starting powder and Y_2O_3 and AlN as sintering additives was liquid phase sintered. Coarse-grained starting powder led to large intergranular phase regions which allowed an accurate determination of the chemical composition by wavelength-dispersive X-ray microanalysis (WDS). When N_2 was used as sintering atmosphere, a N-rich amorphous phase (about 44 at.% N) was identified by WDS to be the main triple-junction phase in the sintered SiC ceramics, while three further crystalline intergranular phases were AlN, $Y_2SiN_4O_3$ and an O-rich phase ($Y_{10}Al_2Si_3O_{18}N_4$). The overall O content was found to be reduced in comparison to the initial powder composition. The incorporation of N from the sintering atmosphere into the intergranular phase and a subsequent carbothermal reduction are believed to be responsible for the removal of O and the formation of the N-rich amorphous phase. © 2002 Published by Elsevier Science Ltd.

Keywords: Electron microscopy; Intergranular phase; Microstructure; SiC; Sintering

1. Introduction

Because of the very significant influence of the intergranular phases on sintering behavior and mechanical properties, quantitative identification of their chemical compositions is of great value for the design of high-performance SiC ceramics. A beneficial additive system has been proven to be Y_2O_3–AlN.[1–3] However, because of the very fine microstructural features of SiC ceramics densified with the additives from this system, which are in the sub-μm range, precise compositional identification of the intergranular phases has not been achieved yet. Therefore, in the present work, a model system was studied using coarse SiC powders (32–160 μm) for liquid-phase sintering, resulting in microstructural features coarse enough for the spatial resolution offered by wavelength-dispersive X-ray spectrometry (WDS). WDS using the scanning electron microscope is an excellent method for the quantitative analysis of chemical compositions because of its high accuracy and ability to quantify light elements (including C, N and O). The intergranular regions are shown to contain large amounts of a N-rich amorphous phase which had not been described up to now.

2. Experimental procedure

The starting materials were a raw Acheson SiC powder (ESK Delfzijl) and fine AlN (Grade C, H. C. Starck) and Y_2O_3 (Grade C, H. C. Starck) powders. The SiC powder had an α:β ratio of 3:2 and a SiO_2 content of 2 wt.%. Two sieves (32 and 160 μm) were used to separate the SiC powder into three fractions with particle sizes of <32 μm, 32–160 μm, and >160 μm. The intermediate fraction, with a volume weighted mean particle size of 64 μm, as measured by laser granulometry (Alcatel, France), was selected for sintering. The compositions of various powder mixtures prepared and the nomenclature used to describe the samples are specified in Table 1. The mixtures were prepared in a Turbula mixer for 72 h using 5 wt.% PVB (polyvinyl butyral) as a binder. The powder mixtures were cold isostatically pressed at 600 MPa into green bodies having a cylindrical shape. The green bodies were then slowly heated, at a rate of 0.16 K/min, to 500 °C in air in order to burn

* Corresponding author. Tel.: +49-711-689-3229; fax: +49-711-689-3131.

E-mail address: ye@aldix.mpi-stuttgart.mpg.de (H. Ye).

0955-2219/02/$ - see front matter © 2002 Published by Elsevier Science Ltd.
PII: S0955-2219(02)00006-7

Table 1
Compositions and sintering conditions of SiC samples

Sample	SiC: additive (vol.%)	Y_2O_3: AlN (mol%)	Sintering condition
C-60AlN–Ar	90:10	40:60	1950 °C, 60 min, 1 MPa Ar
C-80AlN–N2	90:10	20:80	1950 °C, 60 min, 1 MPa N2
C-60AlN–N2	90:10	40:60	1950 °C, 60 min, 1 MPa N2
C-40AlN–N2	90:10	60:40	1950 °C, 60 min, 1 MPa N2
C-25AlN-N2	90:10	75:25	1950 °C, 60 min, 1 MPa N2

Table 2
Characteristics of liquid-phase sintered SiC samples

Sample	Weight loss (%)	Relative density (%)	Content of intergranular phase (Image C point-analysis) (%)
C-60AlN–Ar	2.8	66.8	5.6
C-80AlN–N2	2.2	68.8	16.5
C-60AlN–N2	1.8	67.9	16.0
C-40AlN–N2	1.8	67.4	15.1
C-25AlN–N2	1.6	67	17.6

out the binder. Finally, sintering was performed in a gas-pressure furnace (FCT, Germany) with a graphite heating element in an argon or N_2 atmosphere. The sintering conditions of various samples are summarized in Table 1. After sintering the samples were cooled at a rate of 20 K/min to 1500 °C and then at a rate of ~50 K/min to room temperature.

The densities of sintered samples were measured using Archimedes' method. The theoretical densities of the different compositions were calculated based on the rule of mixtures, by taking the density of SiC (containing 2 wt.% SiO_2) as 3.18 g/cm^3, Y_2O_3 as 5.02 g/cm^3 and AlN as 3.26 g/cm^3. The relative densities were thus available by comparing the measured densities and the theoretical densities. The weight loss during sintering was calculated by weighing the green and sintered bodies. X-ray powder diffractometry (Siemens D5000, Cu K_α radiation) was performed to identify the crystalline phases. Microstructures were observed by using scanning electron microscopy (DSM982, Zeiss) and transmission electron microscopy (JEM 4000EX, JEOL). The content of the intergranular phase was evaluated by analyzing the SEM images using ImageC point-analysis software (Imtronic GmbH). X-ray wavelength-dispersive spectrometry (SX100, Cameca) was used to perform both quantitative electron probe microanalysis with a spatial resolution of 1 μm and elemental mapping with an image size of 576×399 pixels and total scanning time of 20 h. At least 10 points were measured for every phase to obtain statistically meaningful results.

3. Results and discussion

3.1. Overall microstructure and composition

Table 2 gives an overview of the relative density and weight loss after liquid-phase sintering of the materials investigated. The sintering conditions, chosen to allow fine-grained SiC to be sintered to full density,[1–3] lead to a relative density around 67%. Fig. 1 shows the SEM micrographs of the sintered coarse SiC samples. Obviously, the intergranular spaces among the coarse SiC grains were too large to be completely filled by the liquid phase that forms during sintering, thus preventing complete rearrangement of the SiC grains and leaving large pores behind. These large pores are visible in all the samples sintered in Ar and N_2, which explains the low value of the measured relative densities. Although increasing the quantity of additives or extending the sintering time should allow to increase the final density, these methods are not adopted in the present model experiment because of two reasons. First, the sintering conditions should simulate the technologically relevant systems.[1–3] Second, local densification already exists at many locations in the samples as can be seen in Fig. 1. In regions where the liquid phase has completely filled the intergranular spaces, compositional analysis by WDS is feasible.

The relative intergranular phase content is found by evaluating Fig. 1 with a special software (ImageC point-analysis). The bright phase in Fig. 1 is considered as the intergranular phase, the gray phase as SiC grains and the dark phase as holes. The content of the intergranular phase C is calculated by

$$C = \frac{\text{Number of points over bright phase}}{\text{Number of points over bright and gray phases}} \quad (1)$$

The result is shown in Table 2. It is obvious that the SiC sample sintered in Ar (C-60AlN-Ar) contains a smaller amount of intergranular phase (5.6%) than those sintered in N_2 atmosphere (from 15.1 to 17.6%), despite the fact that the green bodies contain the same volume of additives. This is because the decomposition reaction of the additive AlN at the sintering temperature,

$$2\text{AlN} \rightarrow 2\text{Al (l)} + \text{N}_2\text{ (g)} \quad (2)$$

can be efficiently suppressed by a N_2 atmosphere,[2,4] but not in the case of an Ar sintering atmosphere. The decomposition of AlN can even be accelerated in the present model experiment because porous microstructures supply fast channels for releasing N_2 gas and thus encourage the reaction to proceed to the right side. This reason can also serve to explain the lower relative density and higher weight loss of the sample sintered in

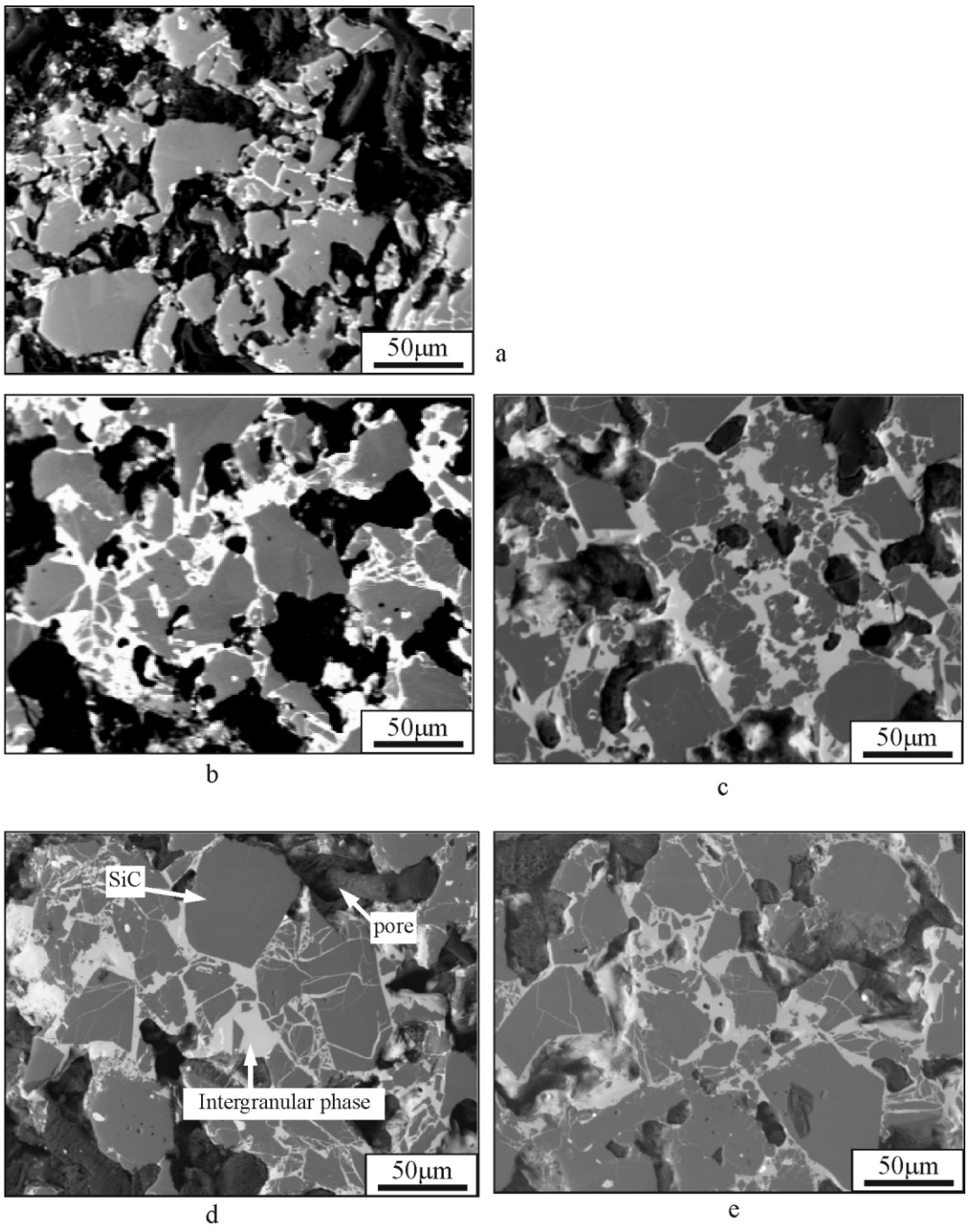

Fig. 1. Backscatted-electron SEM images of liquid-phase sintered coarse SiC: (a) sample C-60AlN–Ar, (b) sample C-25AlN–N2, (c) sample C-40AlN–N2, (d) sample C-60AlN–N2, (e) sample C-80AlN–N2.

Ar, as shown in Table 2. Comparing the SEM micrographs of samples sintered in N_2 (Fig. 1b–e), no obvious structural difference can be found. The change of the ratio of Y_2O_3 to AlN seemingly did not affect the total quantity and distribution of liquid phase in the intergranular spaces.

The XRD pattern of the sample sintered in Ar (C-60AlN-Ar) is shown in Fig. 2a. α-SiC and β-SiC are the major crystalline phases. Minor crystalline phases are identified to be Y_2O_3 (JCPDS Nr. 43–0661[5]) and $Y_{10}Al_2Si_3O_{18}N_4$ (JCPDS Nr. 32–1426) which has frequently been detected when using Y_2O_3–AlN as sintering additives.[1–3] The XRD patterns of samples sintered in N_2 (Fig. 2b) indicate that they also contain α-SiC and β-SiC as major phases and $Y_{10}Al_2Si_3O_{18}N_4$ as minor phase; the difference is that a more N-rich phase, $Y_2SiN_4O_3$ (JCPDS Nr. 30–1460), and AlN (JCPDS Nr. 80–0010) are also identified as minor phases. With the increase of the Y_2O_3 to AlN ratio in the additives, the amount of $Y_{10}Al_2Si_3O_{18}N_4$ increases and that of

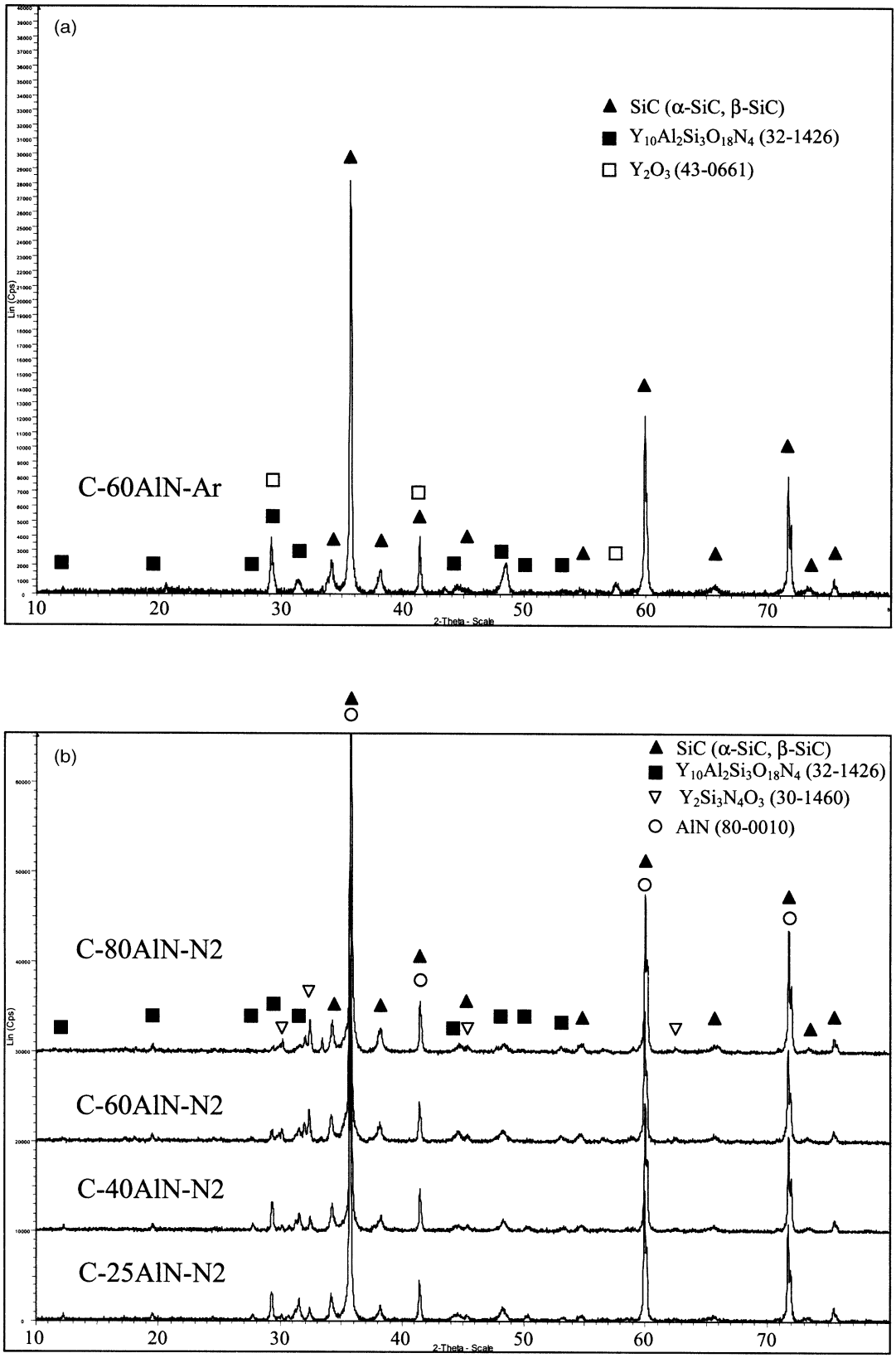

Fig. 2. XRD analyses of liquid-phase sintered coarse SiC: (a) sample sintered in Ar atmosphere, (b) sample sintered in N_2 atmosphere.

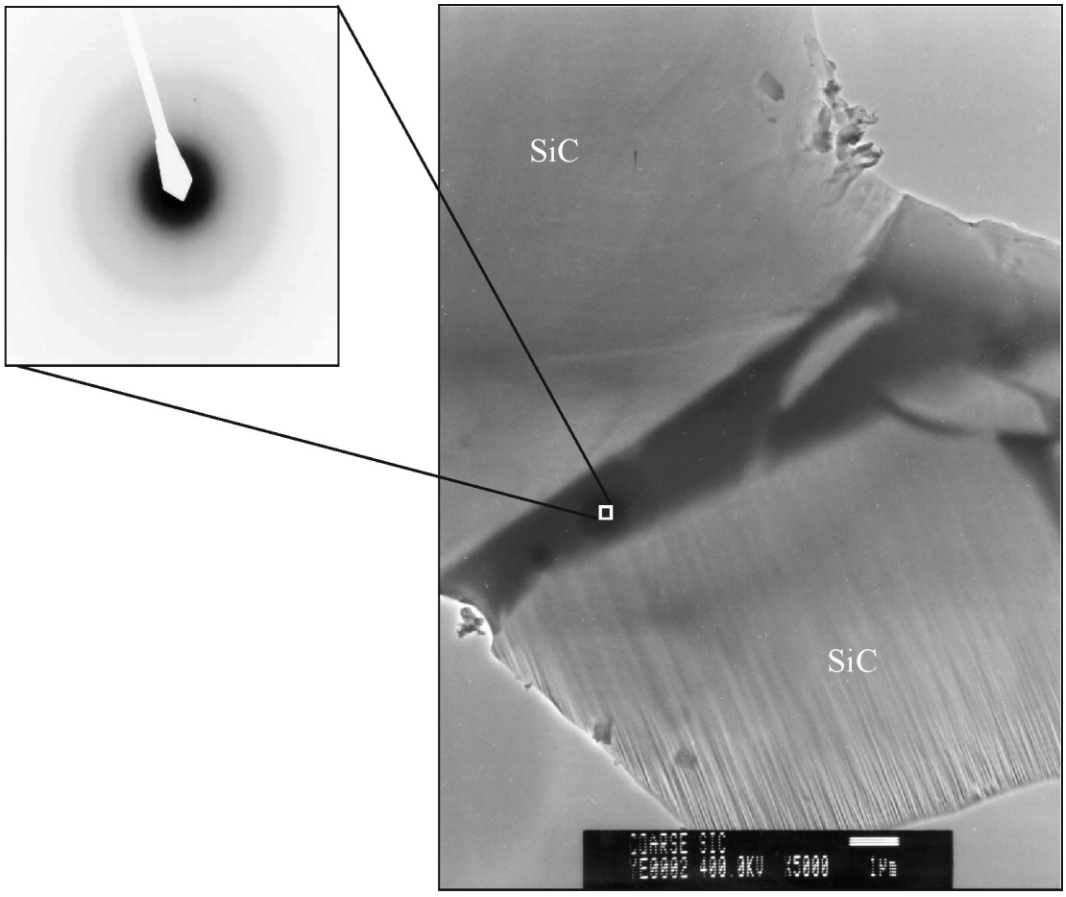

Fig. 3. TEM image and selected-area electron diffraction pattern of the intergranular phase in C-60AlN–N2, showing that the intergranular phase is amorphous.

$Y_2SiN_4O_3$ and AlN decreases (cf. Fig. 2b), but as shown in the SEM images, the total amount of intergranular phases stays nearly constant (cf. Fig. 1 and Table 2).

Transmission electron microscopy was performed as shown in Fig. 3. Selected-area electron diffraction (SAD) was utilized to prove that the main part of the intergranular material was amorphous. In other words, the minor crystalline phases detected by XRD represent only a small portion of the intergranular phase, highlighting the significance of microanalytical methods for identifying the composition of inter-crystalline phases.

3.2. Chemical composition of intergranular phases

In backscattered-electron SEM images (e.g. Fig. 1d), there is a dark gray phase with facetted shapes, which is recognised as SiC, a light gray phase and spots of a bright white phase. Pores appear black. The light gray phase is distributed all over the intergranular regions and constitutes the main part of the intergranular phases. The WDS analysis results on the light gray intergranular phase of the samples sintered in Ar and N_2 are summarized in Fig. 4. An O-rich oxynitride phase, which is commonly observed as the main intergranular phase of liquid-phase sintered Si_3N_4 ceramics,[6] was also identified to account for the main part of the intergranular material in the SiC sample sintered in Ar (see Fig. 4a). In sharp contrast, a new amorphous phase which is rich in N, but depleted of O, was found to occupy much of the intergranular space in the SiC model systems sintered in N_2 (see Fig. 4b). The composition of this new phase remains stable as the ratio of Y_2O_3 to AlN in the additive is changed. Neither the O-rich phase in Fig. 4a nor the N-rich phases in Fig. 4b is corresponding to any crystalline phases identified by XRD analyses (Fig. 2), indicating that this main part of the intergranular phase with a light gray color in SEM images is amorphous, in agreement with the SAD observation (Fig. 3).

It is reasonable to consider that the O-rich phase in Fig. 4a originates from melting of the sintering additives Y_2O_3 and AlN, together with the SiO_2 introduced by surface oxidation of the SiC powder, at the lowest eutectic temperature of 1300–1350 °C which is available in the Y–Si–Al–O–N system.[7,8] According to the solution–reprecipitation sintering mechanism,[9] small SiC grains may dissolve into the liquid intergranular phase and reprecipitate on larger SiC grains when saturation

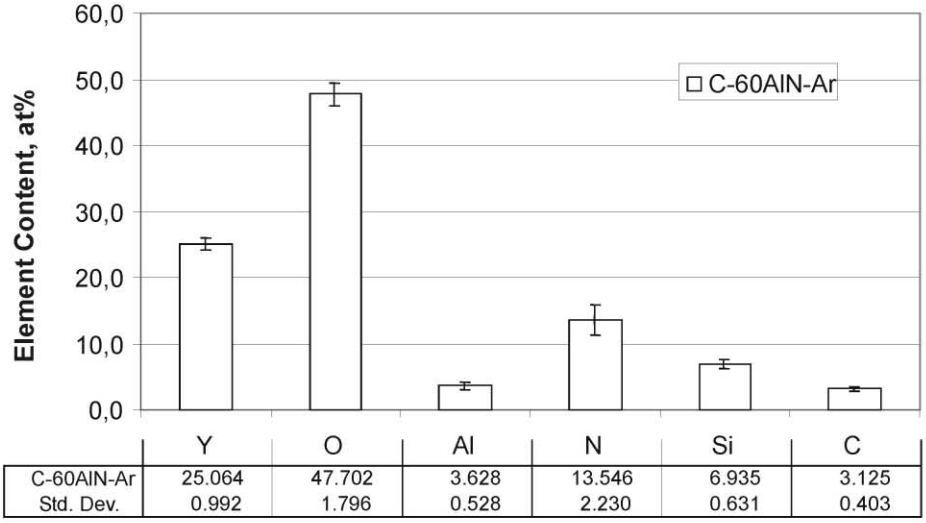

	Y	O	Al	N	Si	C
C-60AlN-Ar	25.064	47.702	3.628	13.546	6.935	3.125
Std. Dev.	0.992	1.796	0.528	2.230	0.631	0.403

a

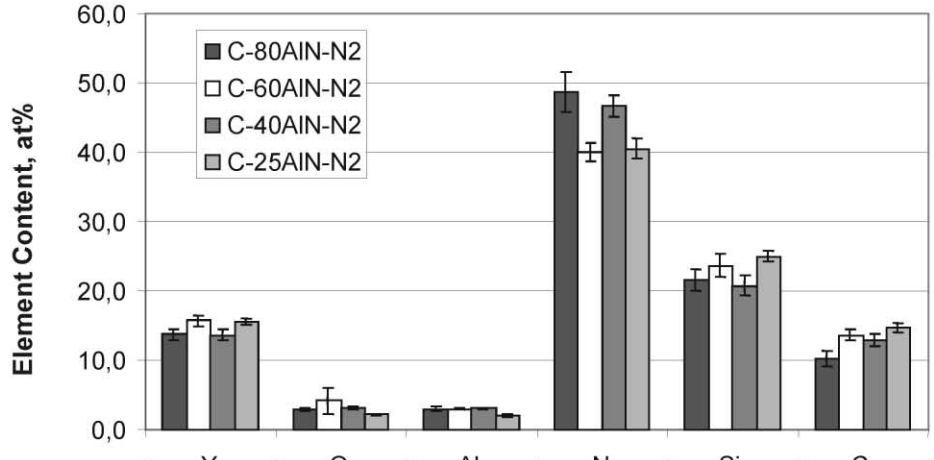

	Y	O	Al	N	Si	C
C-80AlN-N2	13.721	2.855	2.942	48.673	21.595	10.214
Std. Dev.	0.779	0.227	0.335	2.964	1.571	1.194
C-60AlN-N2	15.700	4.130	2.975	39.927	23.650	13.618
Std. Dev.	0.715	1.859	0.151	1.340	1.654	0.830
C-40AlN-N2	13.609	3.143	3.067	46.651	20.714	12.816
Std. Dev.	0.791	0.195	0.152	1.594	1.408	0.920
C-25AlN-N2	15.541	2.212	2.050	40.500	24.971	14.726
Std. Dev.	0.431	0.102	0.183	1.400	0.746	0.695

b

Fig. 4. WDS results on the amorphous intergranular phase of liquid phase sintered SiC, (a) sintered in Ar, (b) sintered in N_2. (Std. Dev. = standard deviation).

of the melt is reached. The overall composition of the melt remains within the glass-forming range of the Y–Si–Al–O–N system,[7,8] although carbon is known to facilitate the crystallization of silicate glasses at high temperatures.[10] Hence, upon cooling, O, Y, N, Al, and dissolved Si and C form the amorphous oxynitride phase with the composition shown in Fig. 4a.

To understand the origin of the N-rich phase in SiC samples sintered in N_2 and its distribution over the intergranular space, WDS maps are helpful. Fig. 5 shows a BSE image together with maps of the element distribution in sample C-60AlN–N_2. Corresponding to the light gray intergranular phase which is visible in Fig. 5, the Y, N and Si maps (Fig. 5b–d) show a homogenous distribution of these elements over the intergranular regions, while O is nearly absent (see Fig. 5f, the regions with bright color marked by circles are due to pores with oxidized surfaces, corresponding to the

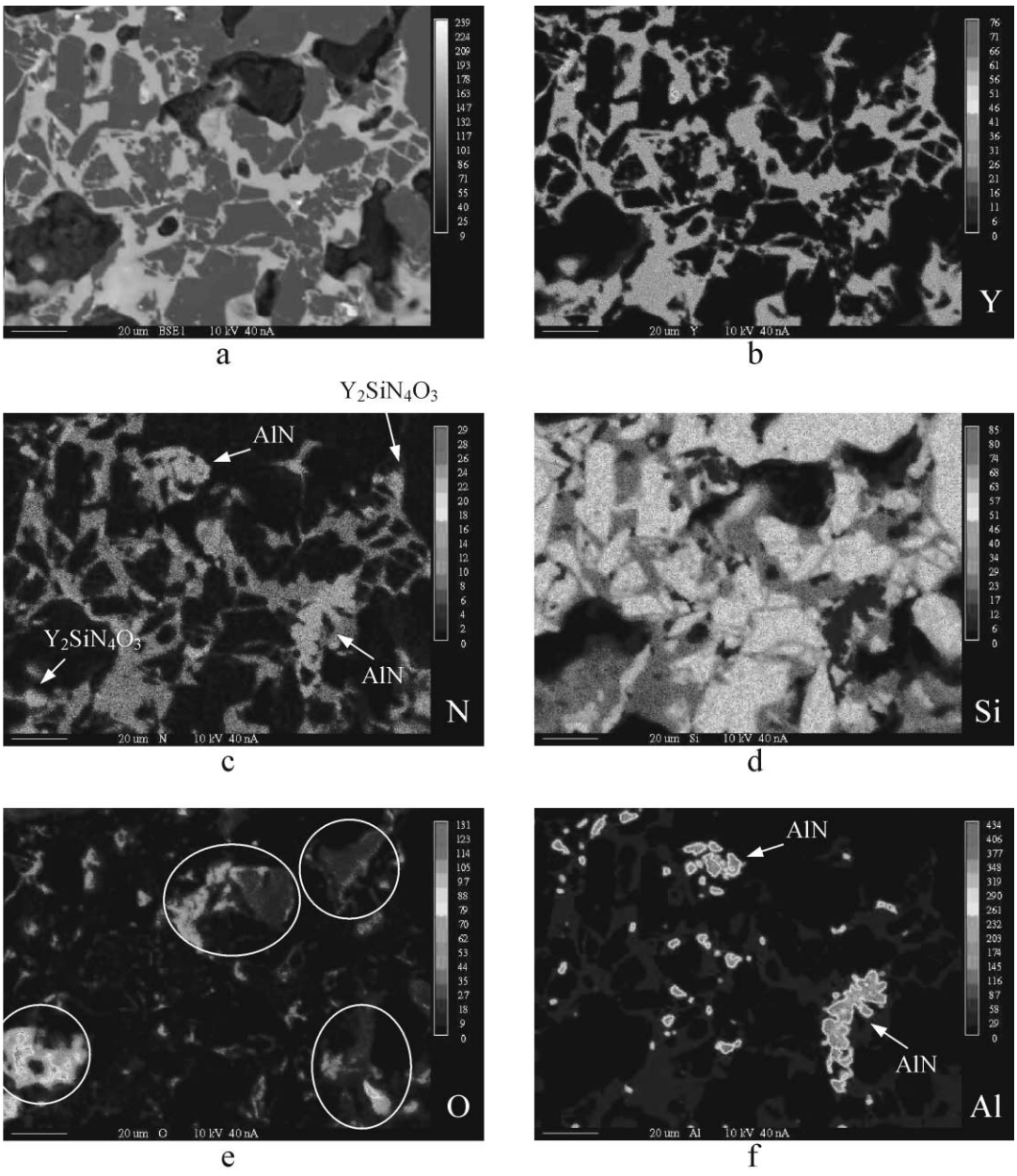

Fig. 5. WDS X-ray maps of the element distribution in C-60AlN–N2: (a) BSE image, (b) Y map, (c) N map, (d) Si map, (e) O map, (f) Al map. The cycles in the O map mark the position of holes, corresponding to the black regions in the BSE image.

black regions in the BSE image, Fig. 5a). The absence of O in the intergranular phase proves the important effect of N_2 as sintering atmosphere on the interfacial chemistry. During the heating period, the sintering behavior should be similar to that in Ar atmosphere, with an O-rich liquid phase forming between the SiC grains. At elevated temperatures, dissolution of N_2 into the liquid intergranular phase causes a sharp increase of its N content, while the decomposition reaction between SiC and oxides, such as SiO_2, which is always present on the surface of SiC powder, causes a decrease in O content, according to equations

$$SiC + 2SiO_2 \longleftrightarrow 3SiO\ (g) + CO\ (g), \quad (3)$$

$$2SiC + SiO_2 \longleftrightarrow 3Si\ (l) + 2CO\ (g). \quad (4)$$

The liquid Si may form bonds to dissolved N to form intergranular phases, which in turn encourages both the decomposition reaction and the dissolution of N. Finally, after a long enough sintering time, the N-rich amorphous phase would occupy the whole intergranular space. Although the low O content places its composition outside the established glass-forming range of the Y–Si–Al–O–N system,[7,8] the amorphous state of the intergranular phase is retained under the present cooling conditions, because high N content leads to a very high viscosity of silicate glass melts.[11] Thus, crystallization is kinetically inhibited.

3.3. Crystalline intergranular phases

Although the main part of the intergranular phases remains amorphous during cooling, local crystallization is always present. Three crystalline intergranular phases, corresponding to the XRD results (Fig. 2b), have been found in the samples sintered in N_2. One of them is AlN, the element distribution of which can be clearly seen in Fig. 5f (Al map) and Fig. 5d (N map). Obviously, the solubility of AlN in the N-rich liquid phase is not high under the present sintering conditions. The Al content in the main intergranular phase always stays at a level of 2–3 at.% (see Fig. 4b). The rest remains as excess crystalline AlN. A second crystalline phase appears as small spots in the N map (Fig. 5d, marked by arrows) but is absent in the Al map (Fig. 5f), indicating that it is a N-rich phase, corresponding to $Y_2SiN_4O_3$ which was identified by XRD. Both these crystalline phases show dark gray color in BSE images (Fig. 5a), similar to SiC grains. In contrast, the third intergranular crystalline phase appears as small bright white spots in BSE images (cf. Fig. 6). The WDS measurement indicates that it is a more O-rich phase. The composition of this phase corresponds to the $Y_{10}Al_2Si_3O_{18}N_4$ phase identified by XRD (Fig. 2). This O-rich crystalline phase ($Y_{10}Al_2Si_3O_{18}N_4$) is always situated inside larger pockets of intergranular material where it is less exposed to the N_2 atmosphere during sintering (cf. Fig. 6).

The identification of the N-rich amorphous phase in the last section and of the N-rich crystalline phase $Y_2SiN_4O_3$ in the present section reveals the strong effect of the incorporation of N on the composition of the intergranular phases. Although using coarse SiC as starting powder causes the model system to stay far away from equilibrium during sintering, it is reasonable to consider that under the same sintering conditions, similar incorporation of N and similar interfacial reactions should happen when fine SiC powders are used for sintering. Therefore, the measured compositions of the intergranular phases in this model experiment can serve as a reference for understanding the intergranular phases in technologically relevant systems sintered from fine powders.

Generally, N-rich glass has a higher glass transition temperature than silicate glass and therefore, softening of the material is shifted to higher temperatures.[6] The design of the additive composition and sintering process to remove all secondary phases in favour of the formation of the N-rich glass can improve the high-temperature strength retention and possibly also the creep resistance significantly.

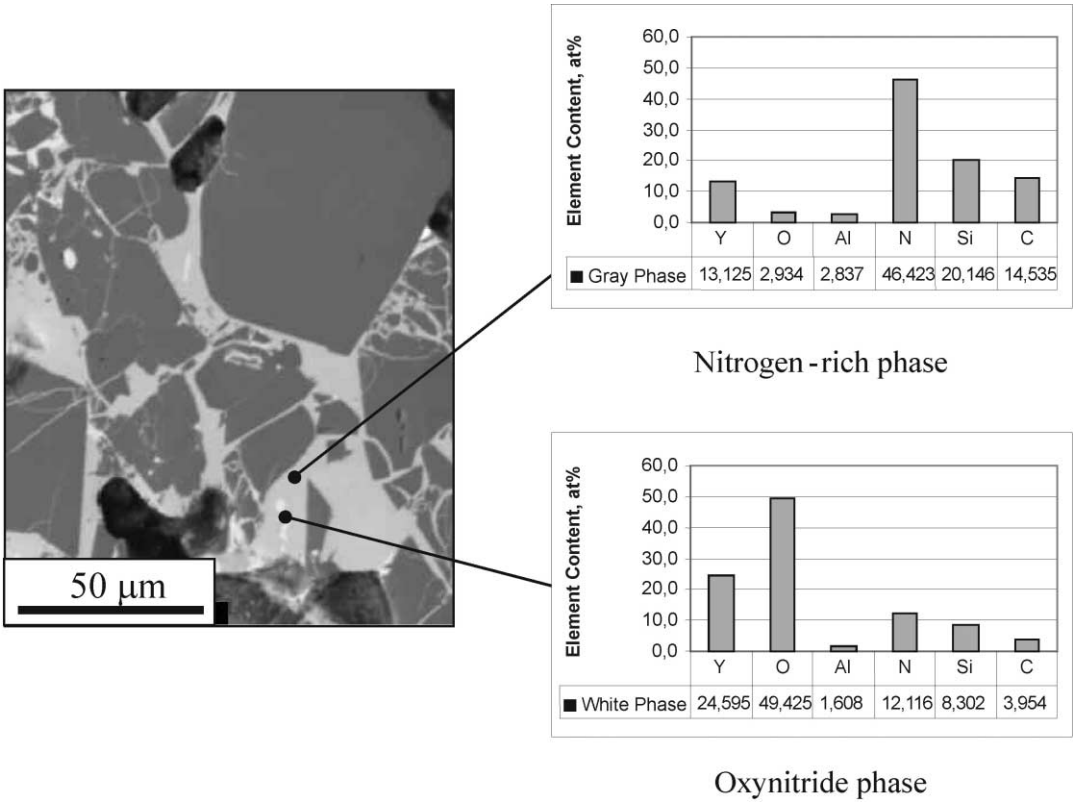

Fig. 6. SEM image and WDS results of C-60AlN–N2, showing the existence of an oxynitride phase with a stoichiometry close to $Y_{10}Al_2Si_3O_{18}N_4$ as a secondary intergranular phase.

4. Conclusion

A nitrogen-rich amorphous phase was identified to be the main intergranular phase in coarse-grained SiC sintered with Y_2O_3–AlN additives in N_2 atmosphere, while three further secondary intergranular phases were AlN, $Y_2SiN_4O_3$, and $Y_{10}Al_2Si_3O_{18}N_4$, respectively. The high incorporation of N_2 from the sintering atmosphere into the intergranular phase leads to an increase of the N content in the intergranular phase and encourages the decomposition reaction between oxides and SiC grains. Together, these two effects can serve to explain the depletion in O and the formation of the N-rich amorphous phase in the intergranular spaces.

Acknowledgements

The authors are sincerely grateful to Mr. Martin Schweizer and Mr. Peter Kopold for help with the sintering and TEM experiments, respectively.

References

1. Keppeler, M., Reichert, H.-G., Broadley, J. M., Thurn, G., Wiedmann, I. and Aldinger, F., High temperature mechanical behaviour of liquid phase sintered silicon carbide. *J. Eur. Ceram. Soc.*, 1998, **18**, 527.
2. Nader M. Untersuchung der Kornwachstumsphänomene an flüssigphasengesinterten SiC-Keramiken und ihre Möglichkeiten zur Gefügeveränderung. Doctoral thesis, University of Stuttgart, Stuttgart, 1995.
3. Rixecker, G., Biswas, K., Wiedmann, I. and Aldinger, F., Liquid-phase sintered SiC ceramics with oxynitride additives. *J. Ceram. Process. Res.*, 2000, **1**, 12.
4. Jun, H.-W., Lee, H.-W., Kim, G.-H. and Song, H. S., Effect of sintering atmosphere on the microstructure evolution and mechanical properties of silicon carbide ceramics. *Ceram. Sci. Eng. Proc.*, 1997, **18**, 487.
5. Joint Committee on Powder Diffraction Standards. ASTM, Swartmore, 1995.
6. Loehman, R. E., Structure, formation, and stability of oxynitride glasses. In *Tailoring of Mechanical Properties of Si_3N_4 Ceramics*, ed. M. J. Hoffmann and G. Petzow. Kluwer Academic Publishers, Dordrecht, 1994, pp. 167.
7. Lewis, M. H., Crystallisation of grain boundary phases in silicon nitride and sialon ceramic. In *Tailoring of Mechanical Properties of Si_3N_4 Ceramics*, ed. M. J. Hoffmann and G. Petzow. Kluwer Academic, Dordrecht, 1994, pp. 217.
8. Seifert, H. J., Lukas, H. L. and Aldinger, F., Development of Si-B-C-N ceramics supported by phase diagrams and thermochemistry. *Ber. Bunsenges. Phys. Chem.*, 1998, **102**, 1309.
9. German, R. M., *Liquid Phase Sintering*. Plenum Press, New York, 1985.
10. Pantano, C. G., Singh, A. K. and Zhang, H., Silicon oxycarbide glasses. *J. Sol-Gel Sci. Tech.*, 1998, **14**, 7.
11. Kaplan-Diedrich, H., Eckebracht, A. and Frischat, G. H., Viscosity and surface tension of oxynitride glass melts. *J. Am. Ceram. Soc.*, 1995, **78**, 1123.